Domains, domain walls and the coercive field of amorphous ferromagnets

H. Kronmüller, B. Gröger

▶ **To cite this version:**

H. Kronmüller, B. Gröger. Domains, domain walls and the coercive field of amorphous ferromagnets. Journal de Physique, 1981, 42 (9), pp.1285-1292. 10.1051/jphys:019810042090128500 . jpa-00209320

HAL Id: jpa-00209320
https://hal.science/jpa-00209320

Submitted on 4 Feb 2008

HAL is a multi-disciplinary open access archive for the deposit and dissemination of scientific research documents, whether they are published or not. The documents may come from teaching and research institutions in France or abroad, or from public or private research centers.

L'archive ouverte pluridisciplinaire **HAL**, est destinée au dépôt et à la diffusion de documents scientifiques de niveau recherche, publiés ou non, émanant des établissements d'enseignement et de recherche français ou étrangers, des laboratoires publics ou privés.

J. Physique **42** (1981) 1285-1292 SEPTEMBRE **1981**, PAGE 1285

Classification
Physics Abstracts
75.60

Domains, domain walls and the coercive field of amorphous ferromagnets

H. Kronmüller and B. Gröger

Institut für Physik am Max-Planck-Institut, Institut für Metallforschung, Stuttgart, F.R.G.

(*Reçu le 23 avril 1981, accepté le 27 mai 1981*)

Résumé. — Les propriétés magnétiques du cycle d'hystérésis des alliages ferromagnétiques amorphes sont essentiellement dues à un couplage magnétostrictif entre l'aimantation spontanée et les contraintes internes. La structure en domaines et l'épinglage des parois sont gouvernés respectivement par des contraintes à grande et à courte distance. Nous avons mis en évidence, comme sources de contraintes élastiques, des dipoles de dislocations dont les champs de contraintes varient en $1/r^2$. On montre que le champ coercitif est déterminé par 4 types d'interactions : 1) épinglage en volume par les sources de contraintes ; 2) fluctuations intrinsèques des constantes matérielles ; 3) irrégularités de surface ; 4) phénomènes de relaxation.

Abstract. — Magnetic properties of the hysteresis loop of magnetostrictive amorphous ferromagnetic alloys are predominantly determined by the magnetoelastic coupling energy between the spontaneous magnetization and internal stresses. Domain structures as well as the pinning of domain walls are governed by long-range and short-range stresses, respectively. As sources of elastic stresses we have detected quasidislocation dipoles exerting stress fields which vary as $1/r^2$. The coercive field is shown to be determined by four types of interactions : 1) volume pinning by stress sources ; 2) intrinsic fluctuations of material properties ; 3) surface irregularities ; 4) relaxation phenomena.

1. **Introduction.** — Amorphous ferromagnetic alloys of transition metals (Fe, Co, Ni) and metalloid atoms (B, P, C, Si, Ge) have been found to exhibit excellent soft magnetic properties which are suitable for technical applications [1-3]. Due to the lack of grain boundaries and any mobile dislocations originally it has been suggested that no pinning forces interacting with domain walls (dws) are present in these materials and consequently the coercive field H_c should be rather small and the permeability, μ, rather high. Nevertheless the real values of H_c and μ are comparable to those of crystalline soft magnetic materials which supports the assumption that amorphous materials should contain defect structures which act as pinning centres for domain walls. Unfortunately the conventional techniques for the study of defects cannot be applied to amorphous materials and therefore new methods must be used in order to obtain informations on defect structures. It has turned out that in particular magnetic techniques are suitable for a study of defect structures. This is related with the fact that the magnetic ground state of the spins in ferromagnetic alloys corresponds nearly to an ideal parallel alignment of the spin in spite of the inhomogeneity of exchange interaction, dipolar fields and local anisotropies. Therefore any inhomogeneity in the spin-system may be connected with a static defect in the amorphous state. It will be shown in the following sections that this leads to a simple picture for the defect structures in amorphous alloys.

2. **Domains and domain walls in amorphous alloys.** —

2.1 DOMAIN PATTERNS IN AMORPHOUS ALLOYS. — By means of the magneto-optical Kerr effect in a series of amorphous alloys the domain structures have been investigated [4-8]. Figure 1 shows a characteristic domain structure of an $Fe_{40}Ni_{40}P_{14}B_6$ alloy [8]. Similarly figure 2 represents the domain patterns of an $Fe_{80}B_{20}$ alloy as observed on two opposite surfaces of an amorphous ribbon which was produced by the spin-quenching technique [9]. One of these latter view graphs is rather low in quality because it has been taken from that side of the ribbon which was in contact with the roller during the preparation. It is well known from previous investigations that this surface of the ribbon is rather rough in comparison to the free

Article published online by EDP Sciences and available at http://dx.doi.org/10.1051/jphys:019810042090128500

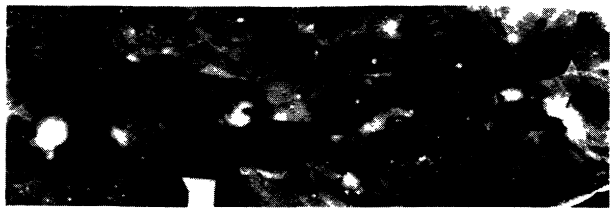

Fig. 1. — Domain structure of the free surface of an $Fe_{40}Ni_{40}P_{14}B_6$-ribbon showing narrow and wide domain patterns.

surface of the ribbon. The domain patterns in figure 1 and figure 2 show two characteristic domain arrangements :

1. Wide and extended wavy laminae of width 10 μm-100 μm and extensions of 200 μm-500 μm.

2. Islands of rather narrow laminae sometimes showing zig-zag lines. These islands have diameters of 50-150 μm.

Comparing both surfaces of the $Fe_{80}B_{20}$ alloy the following conclusions may be drawn :

1. The narrow domains (80 %) on one surface have a counterpart on the opposite surface.

2. Wide, extended laminae appear in the same regions on both surfaces showing small deviations in the detailed arrangement of dws.

The arrangement of domains in general corresponds to a minimum of the magnetic Gibbs free energy, ϕ, of the ferromagnet. Several energies contribute to ϕ :

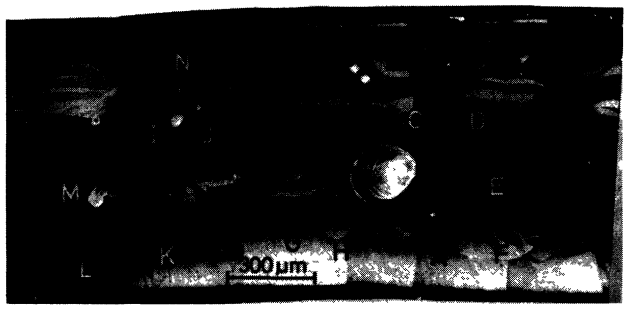

a) Free surface.

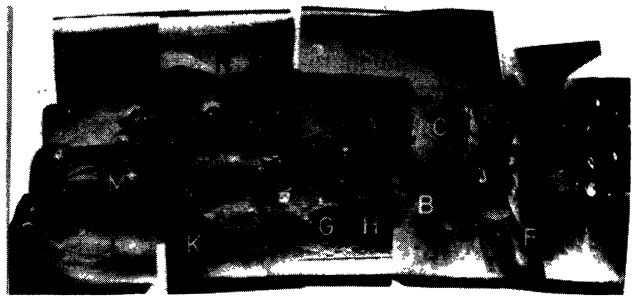

b) Contact side.

Fig. 2. — Domain structures on the free surface and the opposite contact surface of an $Fe_{80}B_{20}$-ribbon. Equivalent domain structures observed on opposite sites of both surfaces are denoted by the same letters.

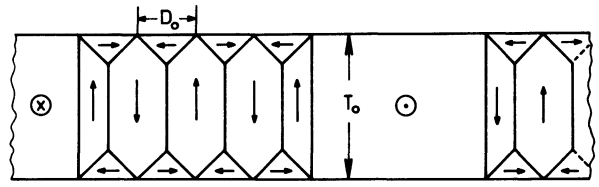

Fig. 3. — Model for the narrow laminae in regions of compressive stresses with stray field-free closure domains.

1. Magnetostatic stray field energy, ϕ_s, due to the demagnetization field.

2. Anisotropy energy, ϕ_a, due to a long-range atomic pair ordering or resulting from the magnetoelastic coupling energy. In both cases the anisotropy energy in a first approximation may be written as

$$\phi_a = K_0 \times \sin^2 \theta . \tag{1}$$

3. Domain wall energy

$$\phi_\gamma = \sum_i \gamma_{B,i} F_{B,i} \tag{2}$$

where $\gamma_{B,i}$ corresponds to the specific wall energy of the i'th dw-type and $F_{B,i}$ to the area of the i'th wall type per unit volume.

The role of these different energies becomes clear if their anisotropy and their orders of magnitude are compared with each other. Considering the maximum values of the different energies we find for $Fe_{80}B_{20}$:

$$\phi_s = 4 \times 10^5 \text{ J/m}^3 , \quad \phi_a = 6 \times 10^3 \text{ J/m}^3 , \quad \phi_\gamma = 60 \text{ J/m}^3 .$$

Here we have assumed a magnetization oriented perpendicular to the ribbon and the material parameters for ϕ_a and ϕ_γ were taken from a previous paper [5]. A first step for a minimization of the total Gibbs free energy is a reduction of ϕ_s by special spin arrangements where magnetic volume as well as surface charges are avoided. The minimization of ϕ_a is obtained if the spontaneous magnetization aligns parallel to the easy axis. If the easy axis lies within the ribbon's plane the domain structure is composed of wide laminae. If the easy axis lies perpendicular to the ribbon's plane the stray field energy would become large. Therefore a closure domain structure develops as shown in figure 3. In figure 4 a domain structure model is shown where the easy axis changes its direction within the cross-section of the ribbon. Within

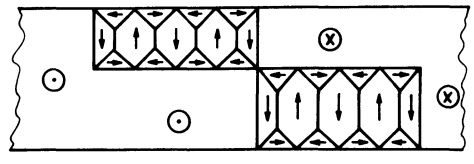

Fig. 4. — Model for the narrow laminae penetrating the ribbon only partially due to a change of easy direction within the ribbon (transition from compressive to tensile stresses).

the closure domains the magnetization aligns perpendicular to the easy axis. This increase of anisotropy energy, however, is small in comparison to the stray field energy required for a perpendicular alignment of M_s.

The regions of narrow domains are coupled to the surrounding wide domains completely stray field free. Within the regions of narrow domains the domain width is given by

$$D_0 = (2\, T_0\, \gamma_B/K_0)^{1/2} \tag{3}$$

where T_0 corresponds to the thickness of the ribbon and γ_B denotes the wall energy

$$\gamma_B = 4 \times \sqrt{AK_0} \tag{4}$$

(A = average exchange constant which may be determined from the spin wave stiffness parameter D). Equations (3) and (4) may be used for a determination of the material parameters

$$\begin{aligned} K_0 &= 64\, AT_0/D_0^4 \\ \gamma_B &= 32\, AT_0/D_0^2 \end{aligned} \tag{5}$$

and the dw width

$$\delta_B = \pi(A/K_0)^{1/2} = \left(\frac{\pi}{8}\right) D_0^2/T_0\,. \tag{6}$$

2.2 Magnetoelastic coupling energy. — In amorphous ferromagnetic alloys the anisotropy energy may have two sources : long-range pair ordering (induced anisotropy) or the magnetoelastic coupling energy of long-range stresses. The first of these anisotropies can be suppressed by a rapid quenching process in the absence of magnetic fields. Due to the rapid quenching process, however, large internal stresses are created because the quenching rate is distributed inhomogeneously over the cross-section of the ribbon. The elastic stress states are simplified by the fact that the thickness of the ribbons ($T_0 \sim 50\,\mu m$) is much smaller than their width (2 000 μm). For such a geometry long-range stresses correspond to planar stress states with zero stress components perpendicular to the ribbon. The magnetoelastic energy for a planar stress state with $\sigma_3 = 0$ may be written as [10]

$$\phi_M = -\tfrac{3}{2}\,\lambda_s \sum_{1,2} \sigma_i\, \gamma_i^2 \tag{7}$$

where σ_1 and σ_2 are the in-plane principal stress components. If the orientation of the spontaneous magnetization $\mathbf{M}_s$ is described by the polar angle φ between $\mathbf{M}_s$ and the ribbon normal, and the azimuthal angle δ between the in-plane component of $\mathbf{M}_s$ and the stress axis X_1 we obtain

$$\phi_M(\varphi, \delta) = -\tfrac{3}{2}\,\lambda_s\, \sigma_1 \sin^2\varphi(1 + a \sin^2\delta) \tag{8}$$

where the in-plane anisotropy factor a is given by $a = (\sigma_2 - \sigma_1)/\sigma_1$. Equation (8) defines two types of easy directions. For positive magnetostriction we obtain :

1. In-plane easy direction, $\varphi = \pi/2$, for $\sigma_{1,2} > 0$. Within the ribbon $\mathbf{M}_s$ orients parallel to $\delta = 0$ for $a < 0$ and parallel to $\delta = \pi/2$ for $a > 0$.

2. Easy direction perpendicular to the ribbon plane, $\varphi = 0$, for compressive stresses $\sigma_{1,2} < 0$. Dws are oriented parallel to $\delta = 0$ for $a > 0$ and parallel to $\delta = \pi/2$ for $a < 0$.

3. The easy directions lie parallel to the ribbons plane if the two stress components have opposite signs, and $\mathbf{M}_s$ orients parallel to the tensile stress axis. In the case of negative magnetostriction the situation for the easy axes is just reversed.

2.3 Domain walls in amorphous ribbons. — In the following we consider dws which show only small curvatures so that we may treat them as planar dws. The arrangement of dws within the ribbons is determined by the long-range part of the anisotropy energy, i.e., by the magnetoelastic energy ϕ_M. According to the results of the previous section in compressive regions the dws align parallel to the axis of the smallest compressive stress component, i.e., for $a > 0$

$$(|\,\sigma_2\,| > |\,\sigma_1\,|)$$

the dws align parallel to the X_1-axis and ϕ_M is given by

$$\phi_M = -\tfrac{3}{2}\,\lambda_s\, \sigma_1 \sin^2\varphi \tag{9}$$

which corresponds to a long-range anisotropy constant $K^{l.r.} = K_0 = -\tfrac{3}{2}\,\lambda_s\,\sigma_1$. Within the dws of the regions of narrow domains the angle rotates from $\varphi = 0$ to $\varphi = \pi$. Neglecting local fluctuations of the anisotropy energy and of the exchange constant A the angle φ obeys the following differential equation

$$2\,A\,\frac{d^2\varphi}{dX_2} - K_0 \sin 2\varphi = 0 \tag{10}$$

with the solutions

$$\sin\varphi = \frac{1}{\cosh(X_2/\delta_0)}\,; \quad \cos\varphi = \tanh(X_2/\delta_0)\,. \tag{11}$$

The parameter δ_0 is related to the dw width according to

$$\delta_B = \pi\delta_0 = \pi\sqrt{A/K_0}\,. \tag{12}$$

The solutions (11) have been found for constant values of A and K_0. In a more realistic model we must take into account spatial fluctuations $\delta A(\mathbf{r})$ and $\delta K(\mathbf{r})$ of the exchange constant and the anisotropy energy. This leads to modifications of the spin distribution given by equation (11). Schematically this is shown in figure 5 where we have indicated the effect of δK by small rotations $\delta\varphi(\mathbf{r})$. It will be shown in section 3 that these intrinsic fluctuations give rise to an intrinsic

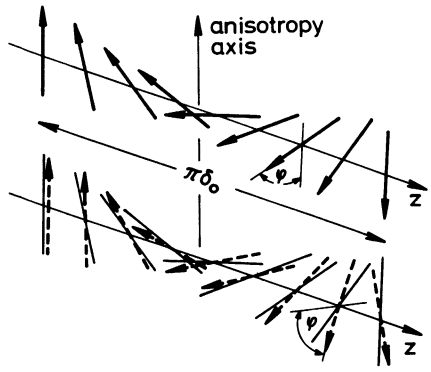

Fig. 5. — Spin structure of an ideal domain wall (upper part), and modification of the spin structure due to locally fluctuating anisotropy and exchange energy.

coercive field of dws in amorphous alloys. The dw widths determined for different materials are shown in table I.

Table I. — *Material constants and domain wall parameters of several amorphous alloys.*

Alloy	K_0 (J/m^3) T = 300 K	A (J/m) T = 4 K	δ_B (nm)	γ_B (J/m^2)
$Fe_{80}B_{20}$	6 × 10^3	5 × 10^{-12}	87	6.9 × 10^{-4}
$Fe_{40}Ni_{40}P_{14}B_6$	0.6 × 10^3	3.1 × 10^{-12}	215	1.7 × 10^{-4}
$Fe_{40}Ni_{40}B_{20}$	1.2 × 10^3	8.1 × 10^{-12}	258	4.0 × 10^{-4}

2.4 ELASTIC STRESSES IN DOMAIN WALLS AND ELASTIC INTERACTION WITH DEFECTS. — As is well known since the work of Rieder [11] the inhomogeneous spontaneous magnetostriction within dws produces an elastic stress field which may be calculated along the concepts of the continuum theory of dislocations [12]. In the case of elastic and magnetostrictive isotropy the elastic strain components in a domain wall with the X_2-axis corresponding to the dw normal are given by (the coordinate axes X_1 and X_3 are oriented parallel respectively perpendicular to the easy axis) .

$$E_{11} = \tfrac{3}{2}\lambda_s \sin^2\varphi\ ;\quad E_{33} = -\tfrac{3}{2}\lambda_s \sin^2\varphi\ ;$$
$$E_{13} = -\tfrac{3}{4}\lambda_s \sin 2\varphi\ . \tag{13}$$

For the elastic stresses we find :

$$\sigma_{11} = 3G\lambda_s \sin^2\varphi\ ;\quad \sigma_{33} = -3G\lambda_s \sin^2\varphi\ ;$$
$$\sigma_{13} = -\tfrac{3}{2}G\lambda_s \sin 2\varphi\ . \tag{14}$$

Defect structures which produce elastic stresses have an elastic interaction with the elastic stresses of the dw. The force acting on the dw may be calculated by the Peach-Köhler formula [13]. If we deal with a dislocation characterized by line elements dl and a Burgers vector **b** the interaction force is given by

$$\mathbf{P}_B = \oint \mathrm{d}\mathbf{l} \times (\boldsymbol{\sigma} \cdot \mathbf{b})\,. \tag{15}$$

Equation (15) is easily modified for the case of dislocation dipoles or point-like defects. If we consider a planar closed dislocation loop with the surface elements d**f** of the area extending over the dislocation loop we obtain for the force acting parallel to the dw normal

$$P_{B,2} = -\int_f [[\mathrm{d}\mathbf{f} \times \nabla] \times \boldsymbol{\sigma} \cdot \mathbf{b}]\,. \tag{16}$$

If the dyadic product d**fb** is introduced as the differential displacement tensor of the defect

$$\mathrm{d}\mathbf{Q} = \mathrm{d}\mathbf{f}\mathbf{b} \tag{17}$$

the interaction force finally may be written as

$$P_{B,2} = -\int_f \mathrm{d}\mathbf{Q}\, \nabla_2 \boldsymbol{\sigma}\,. \tag{18}$$

Equation (18) may be specified to the case of a straight dislocation dipole of length L_3 lying parallel to the X_3-axis which encloses an area DL_3 where D corresponds to the distance between the two dislocations of antiparallel Burger's vector as shown in figure 6. If the dislocation dipole is inclined by an angle ε with respect to the X_1-axis we obtain from (18)

$$P_{B,2} = -Db_1 L_3 \sin\varepsilon\, \nabla_2\, \sigma_{11} - Db_3 L_3 \sin\varepsilon\, \nabla_2\, \sigma_{13}\,. \tag{19}$$

Inserting into (19) the results for σ_{ik} and the spin distribution (10) we obtain

$$P_{B,2} = -3DL_3 G\lambda_s \frac{\sin\varepsilon}{\delta_0} \sin\varphi [b_1 \sin 2\varphi + b_3 \cos 2\varphi]\,. \tag{20}$$

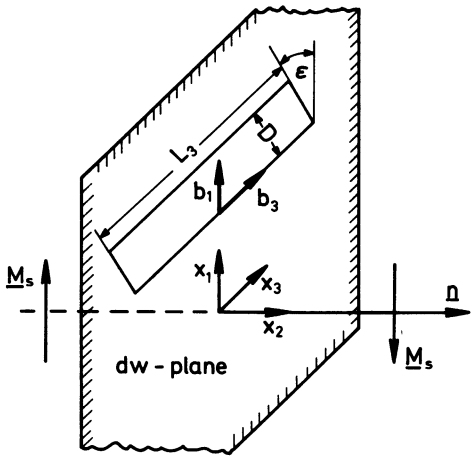

Fig. 6. — Geometry of a quasi-dislocation dipole interacting with a domain wall.

Equation (20) can be written even more explicitly if our results for sin φ and cos φ (see Eq. (11)) are introduced into equation (20). Equation (20) shows that the force vanishes if the Burgers vector lies perpendicular to the dw(b_1, $b_3 = 0$) and if the dipole loop is oriented parallel to the dw($\varepsilon = 0$).

Equation (18) also can be applied to point-like stress centres. If we consider an anisotropic displacement tensor $\mathbf{Q} = \mathbf{I} \cdot Q_0$ ($\mathbf{I}$ = unit tensor) we find

$$P_{B,2} = -Q_0(\nabla_2(\sigma_{11} + \sigma_{33})) = 0 . \qquad (21)$$

According to this result only anisotropic point defects interact with dws in amorphous alloys. Considering a displacement tensor with different components Q_{11} and Q_{33} we obtain

$$P_{B,2} = \frac{1}{\delta_0}(Q_{33} - Q_{11})\, 3\, G\lambda_s \sin\varphi \times \sin 2\varphi$$

$$= \frac{6}{\delta_0}(Q_{33} - Q_{11})\, G\lambda_s \tanh\frac{X_2}{\delta_0}\left[1 - \tanh^2\frac{X_2}{\delta_0}\right]. \qquad (22)$$

3. **Intrinsic coercive field.** — In amorphous ferromagnets with zero magnetostriction it may be suggested that intrinsic fluctuations of the exchange integrals and of the local anisotropy act as pinning centres for dws. These intrinsic interactions between the amorphous structure and dws then determine a lower bound H_c^{min} of the coercive field. Several authors have tried to calculate H_c^{min} by taking into account anisotropy fluctuations only [14-16]. In a more rigorous calculation however, also exchange fluctuations must be considered. For a calculation of H_c^{min} we start from the locally fluctuating contributions $\delta\phi_a$ and $\delta\phi_{ex}$ to the anisotropy and exchange energy, respectively. Introducing the fluctuations δK_i and $\delta\varepsilon_i$ of the anisotropy constant $K(r_i)$ and the exchange energy at position $\mathbf{r}_i$ we obtain

$$\delta\phi_a = \delta K_i \cos^2\theta_i ,$$
$$\delta\phi_{ex} = \frac{1}{2}\delta\varepsilon_i\left(\frac{d\varphi}{dz}\right)^2 . \qquad (23)$$

Here θ_i corresponds to the angle between the magnetization $\mathbf{M}_s$ and the anisotropy axis at position $\mathbf{r}_i$. Within the dw we have $\cos\theta_i(z) = \sin\theta_{0,i}\cos(\varphi - \varphi_{0,i})$ where $\theta_{0,i}$ and $\varphi_{0,i}$ denote the polar angles of the local anisotropy axes with respect to the coordinate system of the dw. Now we may define local pinning forces due to anisotropy and exchange fluctuations

$$P_a = -\frac{d}{dz}(\delta\phi_a) ; \quad P_{ex} = -\frac{d}{dz}(\delta\phi_{ex}) . \qquad (24)$$

According to the statistical potential theory the coercive field H_c^{min} is given by

$$H_c^{min} = \frac{1}{M_s}\frac{1}{\sqrt{2\,F_B}}\left\{\rho_M\left\langle\int_{-\infty}^{\infty}((P_{a,i}(z))^2 + (P_{ex,i}(z))^2)\,dz\right\rangle\right\}^{1/2} \cdot [\ln(L_3/2\,\delta_0)]^{1/2} . \qquad (25)$$

The density of magnetic ions, ρ_M, corresponds to the density of pinning centres. The pointed brackets in equation (28) indicate a volume averaging over the fluctuating quantities δK_i, $\delta\varepsilon_i$, $\theta_{0,i}$ and $\varphi_{0,i}$. After the integration and structure averaging of equation (28) we obtain

$$H_c^{min} = \frac{1}{M_s}\frac{\rho_M^{1/2}}{\sqrt{2\,F_B}}\frac{1}{\delta_0^{1/2}}\left[\frac{8}{15}\langle\delta K_i^2\rangle + \frac{11}{15}\langle\delta\varepsilon_i^2\rangle\cdot(1/\delta_0^4)\right]^{1/2}[\ln(L_3/2\,\delta_0)]^{1/2} . \qquad (26)$$

For soft magnetic materials the fluctuations of the anisotropy energy can be neglected and $\langle\delta\varepsilon^2\rangle$ may be calculated on the basis of a simple nearest neighbour (nn) model. E.g., in the case of NiFePB-alloys the Ni-atoms behave as non-magnetic ions and the total exchange interaction between an Fe-atom and its neighbouring atoms is proportional to the number, n, of nearest neighbour Fe-atoms. In the case of a dense random packing model with 12 nearest neighbour Fe- and Ni-atoms the probability, w_n, to find n nearest neighbour Fe-atoms is given by

$$w_n = \binom{12}{n} C_{Fe}^n (1 - C_{Fe})^{12-n} \qquad (27)$$

where C_{Fe} corresponds to the atomic density of Fe-atoms. Similarly w_n corresponds to the probability for the occurrence of the total exchange integral J_n between n pairs of nn Fe-atoms. By means of equation (27) we may determine the average $\langle\varepsilon_{ex,i}\rangle^2$ making use of the relation $\varepsilon_{ex,n} = \frac{1}{3}r_0^2 J_n$, where r_0 corresponds to the nn distance. A detailed calculation gives

$$\varepsilon_{ex,i} = \frac{1}{9}r_0^4\sum_{n=0}^{12} w_n n^2 J_{FeFe}^2 = \frac{1}{9}r_0^4\cdot 39.0\, J_{FeFe}^2 . \qquad (28)$$

Inserting equation (28) into equation (26) gives

$$H_c^{min} = \frac{1}{3\,M_s}\frac{\rho_M^{1/2}}{\sqrt{2\,F_B}}\frac{J_{FeFe}\,r_0^2}{\delta_0^{5/2}}\left[\frac{39.0\cdot 11}{15}\right]^{1/2}\times$$

$$\times\,[\ln L_2/2\,\delta_0]^{1/2} . \qquad (29)$$

A numerical value of $H_c^{min} = 3 \times 10^{-5}$ Oe is then obtained using $F_B = 6 \times 10^{-5}$ cm^2, $\delta_0 = 10^{-5}$ cm, $M_s = 1\,030$ G, $\rho_M = 4.5 \times 10^{22}$ cm^{-3}, $J_{FeFe} = kT_c/8$, $T_c = 1\,000$ K, (k = Boltzmann constant, T_c = Curie temperature).

This value for H_c corresponds to the absolute minimum value which may be obtained for H_c and which cannot be fallen below even in materials with vanishing local anisotropy.

3.1 MAGNETOSTRICTIVE INTERACTIONS WITH QUASI-DISLOCATION DIPOLES. — The coercive field, H_c, of crystalline materials is determined by grain boundaries and dislocations. In amorphous alloys this kind of defects probably does not exist and therefore small coercive fields are expected. Nevertheless the measured coercive fields are of the order of magnitude of 5-100 mOe, i.e., much larger than intrinsic effects. It is therefore suggested that in amorphous alloys exist inhomogeneities which act as pinning centres for dws. These inhomogeneities correspond to larger defect structures of the amorphous state and it will be the aim of this paper to give an analysis of defect structures of the amorphous state. Previous investigations have shown that mainly magnetostrictive interactions are responsible for finite values of H_c, i.e., these defect structures are characterized by elastic stress fields. This is clearly demonstrated by the dependence of H_c, and other characteristic properties of the hysteresis loop on the magnetostriction. Figure 7 represents H_c, the initial susceptibility χ_0, and the magnetization work, K_{eff}, as function of composition or magnetostriction of the alloying system $Fe_{80-x}Ni_xB_{20}$. With increasing λ_s the coercive field increases where as χ_0 decreases as is expected for the case of magnetostrictive interactions. Only the H_c-value of $Fe_{80}B_{20}$ is an exception probably because this alloy came from Allied Chemical whereas the others were produced by Vacuumschmelze, Hanau. Figure 7 also contains the results for non-magnetostrictive Co-alloys with rather small H_c-values.

From measurements of the field dependence of the high-field magnetization it was derived [5, 17, 18] that the internal stress centres correspond to quasi-dislocation dipoles. For a calculation of the coercive field we use the results of the statistical potential theory derived previously [19, 20]. According to these results the coercive field H_c of a random distribution of quasi-dislocation dipoles of densities ρ_{dip} is related to the pinning force $P_{B,2}$ as given by equation (20) by the following relation :

$$H_c = \frac{1}{M_s}\frac{1}{\sqrt{2\,F_B}}\left[\rho_{dip}\int P_{B,2}^2(z)\,dz\right]^{1/2}\left[\ln\frac{L_2}{2\,\delta_0}\right]^{1/2}, \tag{30}$$

where the last factor takes into account the statistical fluctuations due to the $L_2/2\,\delta_0$ independent positions of the dw within the domain width L_2. In the special case of dipoles with $\varepsilon = \pi/2$ and $b_3 = 0$, $b_1 = b$, and length L_3 we obtain from equation (20)

$$H_c = \frac{.12}{M_s}\frac{1}{\sqrt{30\,F_B}}\,G\lambda_s\frac{\Delta V}{\delta_0^{1/2}}\,\rho_{dip}^{1/2}\,[\ln(L_2/2\,\delta_0)]^{1/2} \tag{31}$$

where $\Delta V = DL_3\,b$ corresponds to the volume contraction due to the quasi-dislocation dipole. From equation (31) we derive for the main temperature dependence of H_c

$$H_c(T) \sim \frac{\lambda_s}{M_s}K_0^{1/4}. \tag{32}$$

For a test of equation (32) in figure 8 we have plotted the quantity $H_c\,M_s/\lambda_s$ *versus* $K_0^{1/4}$ which leads to straight lines [18]. This result may be taken as a proof for the existence of *quasi-dislocation dipoles.* If the magnetostrictive interaction would be due to quasi-dislocations only the quantity $H_c\,M_s/\lambda_s$ would be prop. to $K_0^{-1/4}$ thus leading to a completely different temperature dependence of H_c. A numerical calculation of H_c on the basis of equation (31) leads to the measured H_c-values if the parameters derived for the quasi-dislocation dipoles from high-field suscepti-

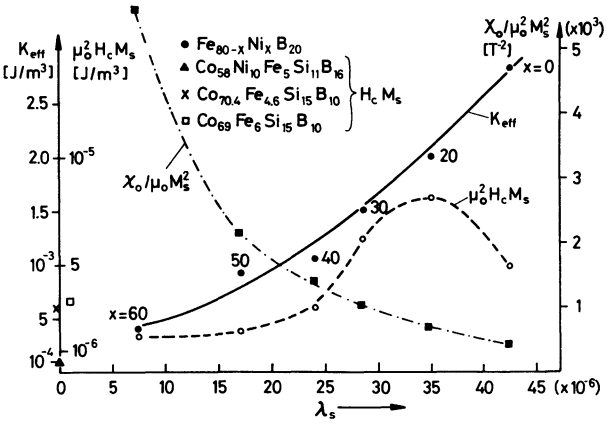

Fig. 7. — The magnetization work, K_{eff}, $H_c\,M_s$ and χ_0/M_s for $Fe_{80-x}Ni_xB_{20}$ alloys and some Co-alloys as a function of λ_s.

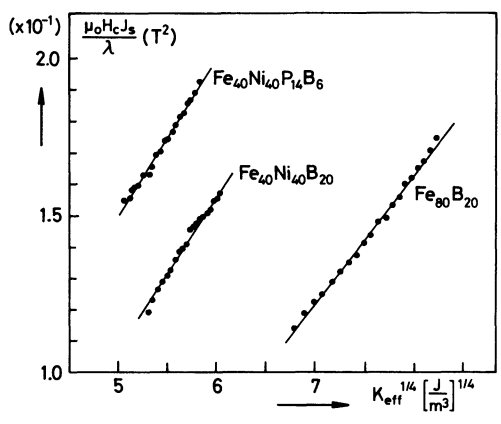

Fig. 8. — Test of the temperature dependence of H_c according to equation (32).

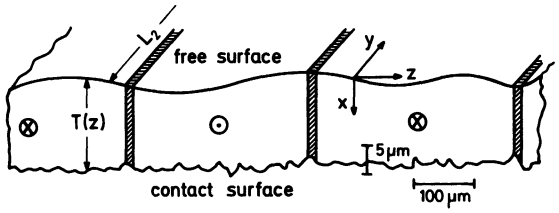

Fig. 9. — Domain walls in a ribbon with fluctuating thickness $T(y, z)$ showing a smooth free surface and a rough contact surface.

bility measurements are inserted [17], [18] ($D_{dip} = 100$ Å; $L_3 = 500$ Å; $b = 2$ Å, $\rho_{dip} = 2 \times 10^{17}$ cm^{-3}, $\delta_0 = 1\,000$ Å, $L_2 = 100$ μm).

3.2 Effects of surface irregularities. — Spin-quenched amorphous ribbons are characterized by surfaces with a natural roughness due to the quenching conditions on the rotating roller. As shown schematically in figure 9 amorphous ribbons produced by the spin-quench technique have a smooth surface on the free surface (off-roller surface) and a rather irregular surface on that side which was in contact with the roller surface. Therefore the ribbon's thickness, T, may be described by a two-dimensional function, $T(y, z)$. Under the action of an applied magnetic field a dw moves through regions of varying cross-sections, i.e., the dw area, F_B, depends on the position of the dw. Accordingly the total wall energy of a planar dw may be written as

$$\phi_\gamma = \gamma_B F_B(z) = \gamma_B L_2 \bar{T}(z), \tag{33}$$

where L_2 denotes the length of the dw and $\bar{T}(z)$ corresponds to the spatially varying average thickness of the ribbon along the dw normal. $\bar{T}(z)$ may be defined as

$$\bar{T}(z) = \frac{1}{L_2} \int_0^{L_2} T(z, y)\, dy, \tag{34}$$

where the integration is performed parallel to the trace of the planar dw with the ribbon's surfaces.

In order to push the dw through the ribbon of varying cross-sections a coercive field of

$$H_c^{surf.} = \frac{\gamma_B}{2 M_s \langle T \rangle} \left\langle \frac{dT}{dz} \right\rangle_{max} \tag{35}$$

is required. Here $\langle T \rangle$ denotes the two-dimensional average of the thickness, $\langle dT/dz \rangle_{max}$ corresponds to the statistical average of the maximum surface gradients. It is obvious then that the surface coercive field is exclusively determined by the rough side of the ribbon where values of $dT/dz \sim 0.1$ may occur. With $\gamma_B = 0.1$ erg/cm^2, ($Ni_{40}Fe_{40}P_{14}B_6$), $M_s = 1\,000$ G, $D = 50$ μm and $\langle dT/dz \rangle_{max} = 0.1$ we obtain

$$H_c^{surf.} = 1 \text{ mOe}.$$

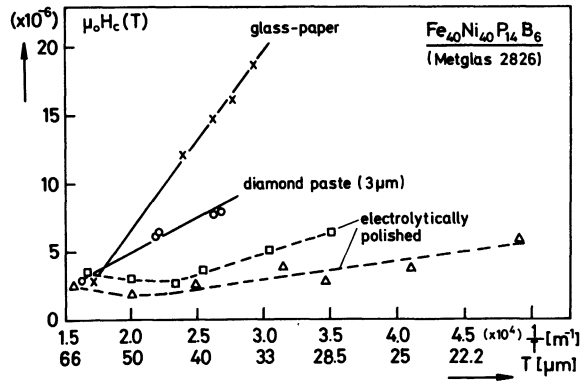

Fig. 10. — The coercive field as a function of the ribbon thickness after different polishing treatments.

For $Fe_{80}B_{20}$ with $\gamma_B = 0.6$ erg/cm^2 we would obtain 6 mOe, i.e., an appreciable contribution to the coercive field. The coercive field due to surface irregularities is characterized by a $1/\langle T \rangle$-dependence which means that $H_c^{surf.}$ increases with decreasing ribbon thickness. This relation has been tested by thinning a $Fe_{40}Ni_{40}P_{14}B_6$-ribbon by means of different techniques. The results are summarized in figure 10. Here it becomes evident that the slopes of the $H_c \rightarrow 1/\langle T \rangle$-plots are largest for a rough surface treatment and are smallest if the ribbon is thinned electrolytically. In all three cases, however, we observe a $1/\langle T \rangle$-dependence as predicted by equation (35). It should be noted that the slopes of the $1/\langle T \rangle$-plots are enhanced due to the strong surface irregularities introduced by the mechanical polishing.

3.3 Influence of magnetic after-effects. — Since the fundamental work of Snoek [21] and Néel [22, 23] it is well known that in crystalline materials the mobility of dws is influenced by thermally activated rearrangements of interstitial impurities, e.g., carbon or nitrogen atoms, within dws. It is suggested that also in amorphous materials atomic rearrangements lead to a structural relaxation giving rise to a stabilization of the dws. Such relaxations may occur by means of the so-called free volume which is stored as empty regions between the ions. The origin of the free volume is due to the different ionic radii of the alloying constituents which prevent the formation of a totally close packed atomic structure. The relaxation process may correspond to a reorientation of atom-pair axes with respect to the spontaneous magnetization or to a reorientation of metalloid atoms which occupy positions corresponding to some kind of interstitial sites. Due to the atomic rearrangements the dw lowers its wall energy. We may describe this process as a lowering of the potential minimum within which the dw is situated. Since the atomic rearrangement occurs by thermally activated processes the stabilization energy of the dw becomes time dependent, and consequently also the contribution of relaxation

processes to the coercive field becomes also a function of time. The additional magnetic field required to push the dw out of its potential minimum is given by

$$H_c^{\text{rel.}}(t) = \text{const.} \frac{\rho_p}{kT} (1 - e^{-t/\tau}) \qquad (36)$$

where ρ_p corresponds to the number of mobile atomic pairs and the relaxation time τ obeys an Arrhenius relation : $\tau = \tau_0 \exp(Q/kT)$. Equation (36) holds if the relaxation process can be described by one unique relaxation time. Actually, however, a spectrum of relaxation times exists [24, 25] leading in general to a more complex relaxation function. The effect of relaxation processes on the unrelaxed coercive field can be estimated from the fundamental relation :

$$\chi_0(t) H_c(t) \simeq \frac{M_s \delta_B}{L_2} \qquad (37)$$

which holds within the framework of the potential theory of the rigid domain wall model [5]. According to equation (37) a relaxation effect, $\Delta\chi$, of the initial susceptibility is related to a decrease, ΔH_c, of the coercive field as follows :

$$\frac{\Delta H_c}{H_c(0)} = -\frac{\Delta\chi}{\chi_0}. \qquad (38)$$

The coercive field due to relaxation effects therefore is given by

$$H_c^{\text{rel.}} = \Delta H_c = -\frac{\Delta\chi}{\chi_0} H_c(0) \qquad (39)$$

where $H_c(0)$ corresponds to the unrelaxed coercive field. Experimentally $(-)\Delta\chi/\chi_0$ was found to vary between 0.05 – 1.0 [24, 25] depending on the annealing conditions of the amorphous alloys. Therefore $H_c^{\text{rel.}}$ may give contributions from 5 %-100 % to the unrelaxed coercive field.

4. **Conclusions.** — 1. Domain patterns are determined by *long-range stresses*. Tensile stresses generate in positively magnetostrictive materials wide and wavy laminae. Compressive stresses result in narrow laminae with an easy direction perpendicular to the amorphous ribbon.

2. Domain wall pinning is due to *short-range stresses* which are produced by quasi-dislocation dipoles.

3. The coercive field is the sum of four terms

$$H_c = H_c^{\text{min}} + H_c^{\sigma} + H_c^{\text{surf.}} + H_c^{\text{rel.}} .$$

Addition of these four terms is possible since the wavelength of the interactions due to short-range elastic stresses (H_c^{σ}), relaxation processes ($H_c^{\text{rel.}}$) and intrinsic fluctuations (H_c^{min}) is $2\,\delta_0$, whereas the wavelength of the surface interactions is of the order of 100 μm.

References

[1] Luborsky, F. E. and Walter, J. L., *IEEE Trans. Mag.* **MAG-13** (1977) 1635.

[2] Hilzinger, H.-R., Mager, A. and Warlimont, H., *J. Magn. Magn. Mat.* **9** (1978) 191.

[3] Luborsky, F. E. and Johnson, L. A., *J. Physique Colloq.* **41** (1980) C8-820.

[4] Kronmüller, H., Schäfer, R. and Schröder, G., *J. Magn. Magn. Mat.* **6** (1977) 61.

[5] Kronmüller, H., Fähnle, M., Domann, M., Grimm, H., Grimm, R. and Gröger, B., *J. Magn. Magn. Mat.* **13** (1979) 53.

[6] Hubert, A., *J. Magn. Magn. Mat.* **6** (1977) 61.

[7] Schröder, G., Schäfer, R. and Kronmüller, H., *Phys. Status Solidi* (a) **50** (1978) 475.

[8] Tsukahara, S., Satoh, T. and Tushima, T., *IEEE Trans. Mag.* **MAG-14** (1978) 1022.

[9] Kronmüller, H. and Fernengel, W., *Phys. Status Solidi* (a) **64** (1981) 593.

[10] Livingston, J. D., *Phys. Status Solidi* (a) **56** (1979) 637.

[11] Rieder, G., *Abh. Braunschw. Wiss. Ges.* **11** (1959) 20.

[12] Kröner, E., *Kontinuumstheorie der Versetzungen und Eigenspannungen* (Springer Verlag, Berlin-Göttingen-Heidelberg-New York) 1958.

[13] Peach, M. and Koehler, J. S., *Phys. Rev.* **80** (1950) 436.

[14] Alben, R., Becker, J. J. and Chi, M. C., *J. Appl. Phys.* **49** (1978) 1653.

[15] Evetts, J. E., Howarth, W. and Gibbs, M. R. J., *Proc. 3rd Int. Conf. Rapidly Quenched Metals*, Met. Soc. London 1978, p. 127.

[16] Fähnle, M. and Egami, T., *J. Magn. Magn. Mat.*, to be published.

[17] Kronmüller, H., *IEEE Trans. Mag.* **MAG-15** (1979) 1218.

[18] Kronmüller, H., *J. Physique Colloq.* **41** (1980) C8-618.

[19] Träuble, H., in *Moderne Probleme der Metallphysik*, vol. **II**, (Springer Verlag, Berlin-Heidelberg-New York) 1966, p. 157.

[20] Kronmüller, H., *Z. Angew. Phys.* **30** (1970) 9.

[21] Snoek, J. L., *Physica* **6** (1939) 161 ; **6** (1939) 591.

[22] Néel, L., *J. Physique Radium* **11** (1950) 49 ; **13** (1952) 249.

[23] Kronmüller, H., *Nachwirkung in Ferromagnetika* (Springer-Verlag, Berlin-Heidelberg-New York) 1968.

[24] Allia, P., Mazzetti, P. and Vinai, F., *J. Magn. Magn. Mat.* **19** (1980) 281.